IOP PUBLISHING JOURNAL OF PHYSICS D: APPLIED PHYSICS

J. Phys. D: Appl. Phys. **40** (2007) 4368–4375 doi:10.1088/0022-3727/40/14/036

Growth of liquid bridge in AFM

Zheng Wei[1,2] **and Ya-Pu Zhao**[1,3]

[1] State Key Laboratory of Nonlinear Mechanics, Institute of Mechanics, Chinese Academy of Sciences, Beijing 100080, People's Republic of China
[2] College of Mechanical Engineering, Beijing University of Chemical Technology, Beijing 100029, People's Republic of China

E-mail: yzhao@imech.ac.cn

Received 1 May 2007, in final form 21 May 2007
Published 29 June 2007
Online at stacks.iop.org/JPhysD/40/4368

Abstract
Capillary forces are dominant in adhesive forces measured with an atomic force microscope (AFM) in ambient air, which are thought to be dependent on water film thickness, relative humidity and the free energy of the water film. In this paper, besides these factors, we study the nature of the 'pull-off' force on a variety of atmospheres as a function of the contact time. It is found that capillary forces strongly depend on the contact time. In lower relative humidity atmosphere, the adhesion force is almost independent of the contact time. However, in higher relative humidity, the adhesion force increases with the contact time. Based on the experiment and a model that we present in this paper, the growth of the liquid bridge can be seen as undergoing two processes: one is water vapour condensation; the other is the motion of the thin liquid film that is absorbed on the substrate. The experiment and the growth model presented in this paper have direct relevance to the working mechanism of AFM in ambient air.

1. Introduction

The invention of the scanning tunnelling and the atomic force microscopes (STM and AFM) provides nanoscience and technology with real space images of atomic scale resolution. In addition, the scanning probe microscope (SPM) can be operated in ambient air. This application of SPM promises to open new chapters in materials science, biology and other research areas. In an AFM measurement, adhesion forces between the AFM tip and the sample are vital for understanding the imaging mechanism. Adhesion forces arise from various types of interfacial forces such as capillary, electrostatic and van der Waals forces. Among these forces, the capillary force is dominant in the nanoscale contact in air. The liquid environment typically yields adhesion forces that are one or two orders of magnitude less than the same measurements made in humid air [1]. Capillary force comes from condensation of water vapour between the substrate and the AFM tip during the contact, when a capillary bridge forms between the tip and the substrate. Capillary condensation tends to occur on hydrophilic surfaces. The equilibrium radius of the capillary bridge meniscus is described by the Kelvin equation [2].

Thundat *et al* [3] observed the dependence of adhesion forces on the relative humidity. The adhesion force was observed by Xiao and Qian [4] to increase first and then decrease with increasing humidity. Xu *et al* [5] verified that, besides relative humidity, the pull-off force depends on the contact time. Such effects were measured by Sedin and Rowlen [6] and the present authors [7]. Tang *et al* [8] studied the effect of relative humidity on the adhesion forces of several inorganic crystals by AFM. The results show that the magnitude of adhesion forces is mainly dependent on the surface free energy of the adsorbed liquid film, but almost independent of the film thickness. Although much effort has been made, the dynamical process of the capillary bridge has not been well understood so far. In this paper, we make a semi-quantitative comparison between our adhesion measurement and theoretical model for different contact times. Our model may shed some light on the dynamical process of the capillary bridge.

2. Experimental

The silicon wafers were treated with a hydrophilic process. Before the experiment, the silicon wafers were sequentially immersed in acetone and isopropanol and thoroughly cleaned

[3] Author to whom any correspondence should be addressed.

in an ultrasonic bath. The cleaned silicon wafers were next immersed in a piranha solution of 98% H_2SO_4 and 30% H_2O_2 ($H_2SO_4 : H_2O_2 = 7 : 3$ by volume ratio) at 80 °C for 150 min. The samples were then rinsed with deionized water for many cycles. Finally, they were baked at 80 °C for 120 min. The water contact angle on the hydrophilic silicon was measured to be ∼30 °. As a result of native oxide and chemical oxide [9], SiO_2 layers were on the surface of the silicon wafer after the hydrophilic process.

Adhesion forces tests were performed with a commercial SPM system (Multimode SPM, Nano-Scope IV, Digital Instruments); Si_3N_4 tips mounted on triangular cantilevers were used to measure the pull-off force. Cantilever spring constants with a nominal force constant of 0.12 N m^{-1} (Digital Instruments) were employed.

Adhesion measurements were performed in the force calibration mode, which is generally used to observe multiple tip–sample interactions while the Z-axis piezo oscillating up and down, and is very useful for checking the tip's 'pull-off' characteristics. During the adhesion measurements, the SPM tip is pushed to the flat surface until the micro-cantilever deformation reaches a fixed value, and then it is pulled away from the surface until it is released. The maximum pull-off force is calculated from the force–displacement curve and defined as the adhesion force. In our experiment, adhesion was measured with the Si_3N_4 tip, and the cantilever upward deformation was limited to 30 nm. To reduce the statistical error, adhesion forces were measured for more than 20 times with the same contact duration, and averages were taken as the final adhesion forces.

3. Results and discussion

3.1. Experimental results

In figure 1, the mean values of the adhesion force measured with an AFM Si_3N_4 tip against hydrophilic silicon are plotted as a function of the contact time. The three curves are the measurements for 65%, 30% relative humidity and for the nitrogen atmosphere. Differences between these cases are easily found from figure 1. The adhesion force for 65% relative humidity increases quickly when the contact time is less than 4 s. Subsequently, the adhesion force increases slowly, approaching the equilibrium state. The adhesion force increases by about 30% from the contact time of 1 μs to that of 16 s for 65% relative humidity. It is the same for 30% relative humidity for a short contact time. However, as the contact time is prolonged, the adhesion force for 30% relative humidity has a strong tendency to increase continuously and increases considerably quicker than for 65% relative humidity. The adhesion force increases by about 10% from the contact time of 1 μs to that of 16 s for 30% relative humidity. However, the change of adhesion force measured in a nitrogen atmosphere is completely different from the first two cases. In order to clearly see the change of the adhesion force, we present the adhesion force profile in a different representation in figure 2, namely, as a function of $\log(t)$, where t is the contact time. No obvious change is found in the whole time range from figure 2, which shows that the adhesion force is not sensitive to the contact time.

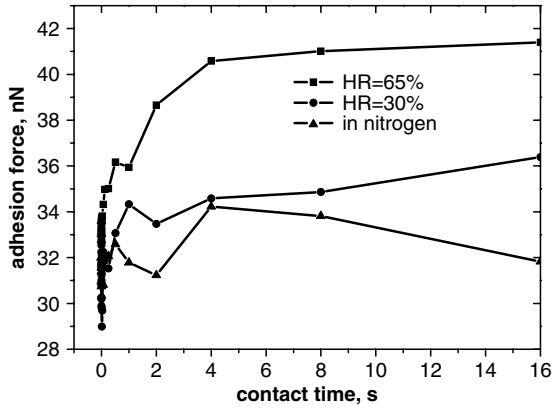

Figure 1. Measured adhesion forces as a function of contact time between Si_3N_4 AFM tip and hydrophilic silicon substrate in three cases: higher relative humidity of 65%, lower relative humidity of 30% and nitrogen atmosphere.

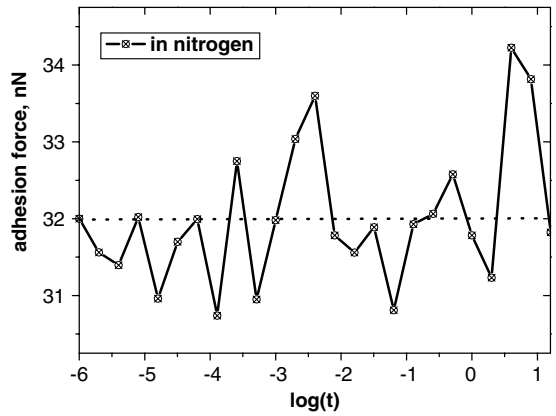

Figure 2. Adhesion forces as a function of $\log(t)$ is plotted for 30% relative humidity, where t is the contact time. The dashed line is the mean value of these adhesion forces.

The adhesion force as a function of the contact time for different humidities was studied by Sedin and Rowlen [6], using a Si_3N_4 AFM tip, with samples being limited to mica. Their results are qualitatively in agreement with ours, namely, no obvious change is found for low relative humidity as the contact time is increased, but an increase of adhesion force is found for higher relative humidity as the contact time increases. Here, we take the nitrogen atmosphere as very low relative humidity. The authors [7] measured the adhesion force as a function of the contact time indirectly for different samples, with the contact time being controlled by adjusting the frequency of the vertical motion of the AFM tip. With relative humidity being limited to 25%, decreasing or unchanging adhesion force was not found in that study.

3.2. Discussion

The capillary force is dominant in the adhesion forces [1], so in our experiment the variation of the adhesion force with time reflects the variation of the capillary force. The capillary force comes from the liquid bridge. Its time dependence suggests that the variation of the adhesion force originates from the formation of liquid bridges between the AFM and the substrate. In [7], a simple mechanism of liquid bridge formation was

presented, but the flow of the liquid thin film was not discussed. Some authors [10, 11] investigated the behaviour of liquid lubricant film through disjoining and capillary pressure.

When two hydrophilic plate surfaces approach each other in a humid environment, the liquid undergoes capillary condensation if the surface separation becomes very close [12, 13]. When an AFM tip is in contact with a substrate, the two facing surfaces, which form a slit, exhibit a much higher adsorption capability because of overlapping adsorption potentials [14–17]. This fact suggests that many water molecules in the ambient air near the slit will be attracted to the contact zone. This process in a small zone is called water condensation, and the condensed water between the AFM tip and the substrate is called a water bridge or a meniscus. The equilibrium problems of capillary condensation have been studied extensively using the surface force apparatus (SFA) [18, 19]. The growth and disappearance mechanisms of lateral microscopic liquid bridges of three hydrocarbon liquids in slit-like pores were studied by Maeda *et al* [20]. In [21], a model was presented on the dependence of the sliding friction on partially hydrophilic and hydrophobic surfaces, which may perfectly reproduce the measured humidity and velocity. A diffusion model was presented to study the kinetic growth of the liquid bridge based on Langmuir's theory of droplet growth [22]. A 'switching' model was presented to include the disjoining pressure and take into account the influence of liquid films adsorbed on the surface in AFM experiments [23]. AFM pull-off experiments performed in air show that stretched nanoscopic water bridges are in mechanical equilibrium but not in thermodynamic equilibrium. The experimental findings were explained by a theoretical model that considers constant water volume and decrease of water meniscus curvature during meniscus stretching [24]. However, the physical justification for such behaviours is not so obvious. So it is of importance to investigate the growth mechanism of the liquid bridge for a better understanding of the relationship between the adhesion force and the contact time.

Among many studies on the growth mechanism of the liquid bridge, the kinetic process of the growth of the liquid bridge has not been paid enough attention. Here, we attribute the growth of the liquid bridge to the water vapour condensation and the motion of the thin liquid film. In air, it is well known that a thin liquid film composed mostly of water adsorbs on surfaces [25]. Due to the presence of the thin film of adsorbed water layers, a liquid bridge forms around the sphere and grows with time until equilibrium establishes [10]. The growth mechanism of the water bridge between the AFM tip and the substrate is shown schematically in figure 3. So besides the condensation of water vapour, the flow of thin liquid film on the substrate to the contact zone might also be a factor in the formation of a liquid bridge. Although the condensation of water vapour and the motion of liquid film are assumed to form the liquid bridge, the actual physical process of these growth mechanisms is unclear.

3.2.1. The time of water condensation to form liquid bridge. The rate of growth of capillary condensates was studied through a model of limited diffusion based on Langmuir's theory of droplet growth [22]. In their model, the diffusion equation is in a steady state. However, the real diffusion is in an unsteady state. This process is very short because the thermal vibration of water vapour molecules is fast. But the water molecules which are slightly far away from the contact zone could not be adsorbed to the slit quickly because their diffusion takes time [26]. So the equilibrium time of the liquid bridge is related to the diffusion time of water vapour from outside to the contact zone. In figure 3(*a*) is shown a schematic diagram of the growth mechanism of a water bridge between the AFM tip and the substrate. The water vapour diffusion can be described by the diffusion equations and solved by various numerical methods, provided that the diffusion coefficients are known. Three distinct transport mechanisms may operate separately or jointly: molecular diffusion (ordinary diffusion), Knudsen diffusion and surface diffusion. Although each individual mechanism is reasonably well understood, it is not always easy to make an accurate prediction of the total diffusivity because it depends strongly on the structure character. Using the elementary kinetic-molecular theory [26], the mean free path of the vapour molecules in our measurements is estimated to be approximately 100 nm, which is smaller than the distance between the confining walls of the pore at the position of the liquid–vapour interface of the condensate in AFM. In this case, the collisions of water molecules against the AFM tip and the substrate provide the main diffusion resistance. Therefore, the Knudsen diffusion is the main diffusion mode.

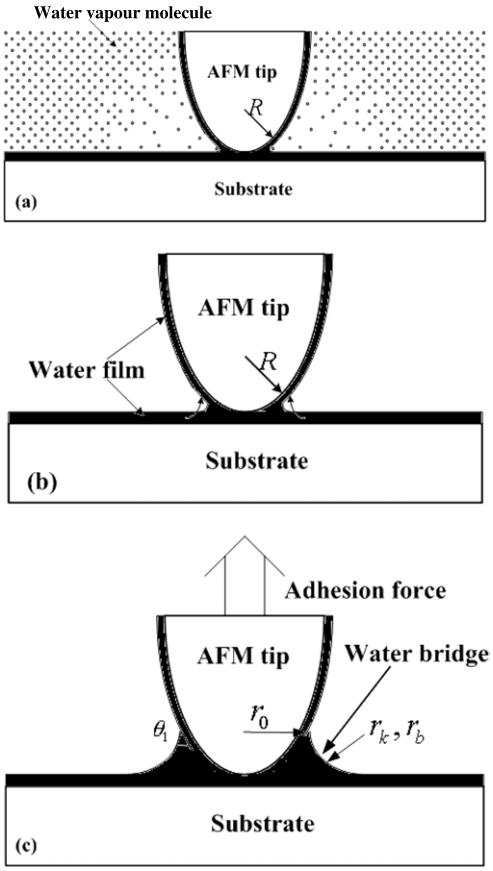

Figure 3. A schematic diagram of the two growth mechanisms of the water bridge between the AFM tip and the substrate. (*a*) Water vapour condensation in the slit around the contact zone. (*b*) The motion of liquid film due to the action of meniscus pressure and disjoining pressure. (*c*) The liquid bridge in equilibrium.

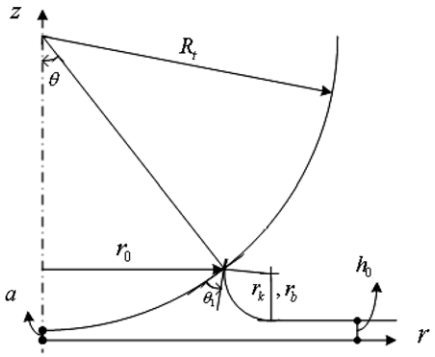

Figure 4. A schematic diagram of the growth formation of water bridge between tip and substrate in air at room temperature, R is the radius of curvature for the AFM tip. A cylindrical coordinate is introduced. The thickness of the water thin film on the substrate is $h = 0.5$ nm; the two contact angles are 0. The AFM tip is simplified as a single asperity with a radius $R_t = 50$ nm.

In the classical Knudsen theory, the diffusion coefficient D is given by Dushman [27] as $D = (2/3)d((2RT)/(\pi M))^{1/2}$, where d is the radius of the pore, R the universal gas constant, T the absolute temperature and M the molar mass of water. In our AFM test, we take $d = 1$ nm, $T = 293$ K, so $D \sim 2 \times 10^{11}$ nm^2 s^{-1}.

A simple analysis is as follows. The coordinate system is shown in figure 4. The diffusion equation is written as

$$\frac{\partial n}{\partial t} = D\Delta n = D\left(\frac{\partial^2}{\partial r^2} + \frac{1}{r}\frac{\partial}{\partial r}\right)n, \tag{1}$$

with the boundary and initial conditions as

$$n|_{r=r_0} = n_l, \tag{2}$$

$$n|_{t=0} = n_\infty, \tag{3}$$

where n is the concentration of the water vapour, D the Knudsen diffusion coefficient, n_∞ the concentration of the water vapour far away from the liquid bridge and n_l the concentration of the water vapour at the interface of the liquid bridge and water vapour, that is controlled by the saturated vapour pressure near the interface.

From the gas molecular motion theory [26]

$$n = \frac{Np}{RT}, \tag{4}$$

and Kelvin equation [2]

$$r_k = \frac{\gamma v_m}{RT\ln(p/p_s)}, \tag{5}$$

we can obtain the relationship between the saturated vapour pressure of the liquid–bridge interface and the radius of the liquid bridge, that is

$$n_l = \frac{N}{RT}p_s \exp\left(\frac{\gamma v_m}{RTr_k}\right). \tag{6}$$

Here, N is the Avogadro's number, p is the water vapour pressure, γ is the surface tension of water, v_m is the molecular volume of water, p_s is the saturated vapour pressure and r_k is the Kelvin radius of the interface.

With a variable $\tilde{n} = -n+n_\infty$, equations (1), (2) and (3) are transformed into another problem [28,29]. Finally the solution to our problem is obtained as

$$n(r,t) = n_l - (n_\infty - n_l) \times \frac{2}{\pi}\int_0^\infty e^{-D\xi^2 t}\left(\frac{J_0(\xi r)Y_0(\xi r_0) - Y_0(\xi r)J_0(\xi r_0)}{J_0^2(\xi r_0) + Y_0^2(\xi r_0)}\right)\frac{d\xi}{\xi}. \tag{7}$$

Then

$$\left.\frac{\partial n(r,t)}{\partial r}\right|_{r=r_0} = (n_\infty - n_l) \times \frac{4}{\pi^2 r_0}\int_0^\infty e^{-D\xi^2 t}\frac{d\xi}{\xi[J_0^2(\xi r_0) + Y_0^2(\xi r_0)]}, \tag{8}$$

where $J_0(n)$ and $Y_0(n)$ are, respectively, the Bessel functions of the first and second kinds of zero order and r_0 is defined in figure 4.

From Fick's first law, we obtain the rate of the adsorbed water of the condensation bridge,

$$Q = \left|\frac{dm}{dt}\right| = DA_b\left(\frac{dn}{dr}\right) = DA_b(n_\infty - n_l) \times \frac{4}{\pi^2 r_0}\int_0^\infty e^{-D\xi^2 t}\frac{d\xi}{\xi[J_0^2(\xi r_0) + Y_0^2(\xi r_0)]}, \tag{9}$$

where A_b is the area of the liquid bridge, so

$$A_b = 2\pi\int r\,dz \approx 2\pi R_t \sin\theta\int dz \approx 2\pi R_t \sin\theta\,[R_t(1-\cos\theta) + a - h_0], \tag{10}$$

where R_t is the radius of the AFM tip.

From the geometric relation, the liquid volume is (see appendix)

$$V = \tfrac{2}{3}\pi R_t(r_k + h_0 - a)^2. \tag{11}$$

We assume that all the condensation water increases in volume and so we have

$$\rho\frac{dV}{dt} = \frac{Q}{N}M, \tag{12}$$

where ρ is the density of water. Then,

$$\rho\cdot\frac{4}{3}\pi R_t(r_k + h_0 - a)\frac{dr_k}{dt} = DA_b\frac{(n_\infty - n_l)}{N}\cdot M \times \frac{4}{\pi^2 r_0}\int_0^\infty e^{-D\xi^2 t}\frac{d\xi}{\xi[J_0^2(\xi r_0) + Y_0^2(\xi r_0)]} = DA_b\frac{Np_s}{RT}(H_r - e^{(\gamma V)/(RTr_k)})\cdot\frac{M}{N} \times \frac{4}{\pi^2 r_0}\int_0^\infty e^{-D\xi^2 t}\frac{d\xi}{\xi[J_0^2(\xi r_0) + Y_0^2(\xi r_0)]}. \tag{13}$$

From a simple geometry (suppose $\theta_1 = 0$), the radius of the liquid bridge is

$$r_k = \frac{R_t(1-\cos\theta) + a - h_0}{1+\cos\theta}, \tag{14}$$

where $\theta = \arcsin(r_0/R_t)$.

Using equation (13), the radius of the liquid bridge as a function of contact time can be calculated. The result is shown in figure 5. It is seen that the equilibrium time is ~1 ms.

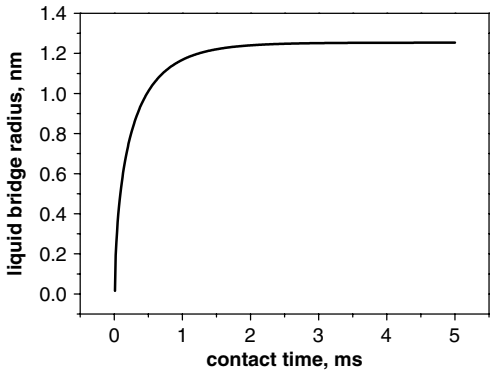

Figure 5. The relationship between the radius of the liquid bridge resulted from the water vapour condensation and the contact time.

3.2.2. The motion of liquid film. In [10], the concepts of disjoining and capillary pressure are applied to analyse the behaviour of thin liquid film on the surface. A thin liquid film has a pressure associated with it that is the sum of the disjoining pressure, which represents the energy of interaction of the film with the underlying substrate, and the capillary or Laplace pressure, which represents the work done to form a curved liquid surface. By equating pressures in the liquid film at different locations, the equilibrium distribution of liquid on a surface can be determined. In our experiment, the capillary length [30] $\kappa^{-1} = \sqrt{\gamma/\rho g}$ for water is about 2.7 mm. Here γ is the surface tension, ρ the liquid density and g the acceleration of gravity. We neglect the influence of gravity because the typical size of the system is small compared with the capillary length. The amount of flow experienced by a liquid film can be expressed by [10]: Flow = (conductance of the film)×(pressure gradient).

The pressure gradient or force per unit volume determines the driving force of the flow. In AFM systems, two types of pressure gradients or forces are present to drive the liquid film flow:

(a) disjoining pressure gradients due to a gradient in film thickness and
(b) capillary pressure gradient.

Furthermore, we consider the liquid film as a Newtonian fluid, the equation of motion derived from the Navier–Stokes equation for an infinitesimal volume element is [10]

$$-\eta\frac{\partial^2 v_r}{\partial z^2} = \frac{\partial \Pi}{\partial r}, \tag{15}$$

where η is the viscosity of the liquid, v_r the velocity of the volume element in the r direction and Π is the disjoining pressure. Applying the boundary conditions of no slippage of liquid at the solid–liquid interface and no air shear or other stress at the liquid–air interface,

$$\begin{cases} v_r = 0, & z = 0, \\ \dfrac{\partial v_r}{\partial z} = 0, & z = h, \end{cases} \tag{16}$$

where h is the thickness of the thin film on the substrate. Thus

$$v_r = -\frac{1}{\eta}\frac{\partial \Pi}{\partial r}\left(\frac{z^2}{2} - hz\right). \tag{17}$$

Then the flow amount is

$$q = \int_0^h v_r \,\mathrm{d}z = \frac{h^3}{3\eta}\frac{\partial \Pi}{\partial r}. \tag{18}$$

If it is assumed that the disjoining pressure comes from the van der Waals interactions [10], i.e. $\Pi = A/6\pi h^3$, then

$$q = -\frac{A}{6\pi\eta h}\frac{\partial h}{\partial z}, \tag{19}$$

where A is the related Hamaker constant.

The volume of the liquid bridge is

$$V = \tfrac{2}{3}\pi R_t r_b^2. \tag{20}$$

The growth of the liquid bridge can be expressed as

$$\frac{\mathrm{d}V}{\mathrm{d}t} = q \cdot 2\pi r_0, \tag{21}$$

where $r_0 = R_t \sin\theta$, as shown in figure 3.

For a liquid bridge at equilibrium with the liquid film on the substrate, the capillary pressure of the liquid bridge will be equal to the disjoining pressure of the film [10], so

$$p_c = \frac{\gamma}{r_b} = \frac{A}{6\pi h^3}, \tag{22}$$

and

$$r_b = \frac{6\pi\gamma h^3}{A}. \tag{23}$$

Then we get

$$\frac{\partial h}{\partial t} = c\frac{\partial h}{\partial r}, \tag{24}$$

$$c = \frac{A^3 r_0}{432\pi^3 R_t \eta \gamma^2 h^6}. \tag{25}$$

We assumed for the liquid film $R_t = 50$ nm, $h_0 = 0.5$ nm [25], $\eta = 0.1$ Pa s [31] and $A = 1.6\times10^{-21}$ J [32]. The equilibrium radius of the liquid bridge is $r_b = 6\pi\gamma h_0^3/A$. Then the water volume that is needed to fill in the liquid bridge is about $V = \frac{2}{3}\pi R_t r_b^2$. The depleted zone is $\sqrt{V/\pi h_0} = \sqrt{(2R_t r_b^2)/(3h_0)} = r_b\sqrt{(2R_t)/(3h_0)}$, so the motion time of liquid film is of the order

$$t \sim \frac{r_b}{c}\sqrt{\frac{2R_t}{3h_0}}. \tag{26}$$

So the equilibrium time is ~4.14 s.

Another correction takes into account the fact that the effective viscosity η of a liquid film might be different from that of the bulk liquid. Experimentally, it is often observed that liquid films of molecular dimensions have viscosities much higher than bulk liquids. An increase in viscosity with decreasing film thickness would tend to slow the flow [10].

The above model shows that the liquid bridge results from the water vapour condensation and the motion of the liquid thin film. During the growth of the liquid bridge, the equilibrium time of condensation of water vapour is much shorter than the equilibrium time of the motion of the thin liquid film, which is absorbed by the substrate and the AFM tip.

3.2.3. The pull-off force between the AFM and the substrate. In general, the adhesion force between an AFM tip and a sample surface should include the capillary force (F_c) as well as the solid–solid interactions, consisting of van der Waals forces (F_{vdW}), electrostatic forces (F_E) and the chemical bonding force (F_B) [33]

$$F_{adhesion} = F_c + F_{vdW} + F_E + F_B. \tag{27}$$

Since the tip and the sample stay in air for a relatively long time (of the order of a few hours), no net charges are expected to remain. Thus, $F_E = 0$ [4]. The chemical bonding force can also be neglected, since the surfaces of the tip and the sample are saturated with chemical bonds. Thus, no ionic or covalent bonds are expected to form during contact [4]. We shall then focus on the first two terms of equation (27).

For a sphere/plane geometry, the van der Waals force is given as [2]

$$F_{vdW} = \frac{AR_t}{6a^2}, \tag{28}$$

where A is the Hamaker constant, which depends on the medium where the two objects stay. For a Si_3N_4/SiO_2 contact, if the medium is air, $A = 10.38 \times 10^{-20}$ J [4]; if the medium is water, $A = 1.6 \times 10^{-21}$ J [32]. According to Israelachvili [2], the separation a for most solid contacts can be taken as ~2 Å, $R_t = 50$ nm, we obtain $F_{vdW}^{air} \approx 22$ nN and $F_{vdW}^{water} \approx 0.34$ nN. Here, the adhesion force in the nitrogen atmosphere of our test is larger than F_{vdW}^{air}, and the adhesion force in 30% and 65% relative humidity is equal to $F_{vdW}^{water} + F_c$. So, the variation of the adhesion force with the contact time is the variation of the capillary force.

From the water condensation analysis, we assume that a liquid bridge is formed instantaneously. The radius of the liquid bridge at thermal equilibrium is given by Kelvin equation [2]. Due to the existence of liquid film on the substrate, the interaction between the disjoining pressure in the thin liquid film and the capillary pressure in the liquid bridge drives some water from the thin film into the liquid bridge. Therefore, the liquid bridge will continuously grow until a new equilibrium is achieved. Based on the above calculation, it can be concluded that the equilibrium for thin film takes a much longer time than for water vapour condensate.

With the model of liquid bridge growth in AFM, we will compare the experimental result with the growth model and demonstrate that our model is applicable to the growth process of the liquid bridge in the AFM test.

Figure 1 shows the dependence of the adhesion forces in various atmospheres on contact time. For a long contact time (longer than 4 s), the adhesion force is almost constant. One can easily understand that the liquid bridge tends to equilibrium when the contact time is long enough. We may take 4 s as the equilibrium time for 65% relative humidity in our AFM measurement. This time is close to the time that is needed for the liquid thin film to form a liquid bridge. In our model, the time is about 4.14 s. A sharp increase of adhesion force for 65% relative humidity is seen when the contact time is restricted to a shorter time in figure 1. We may imagine that when the contact time is fairly short, the water vapour condensation

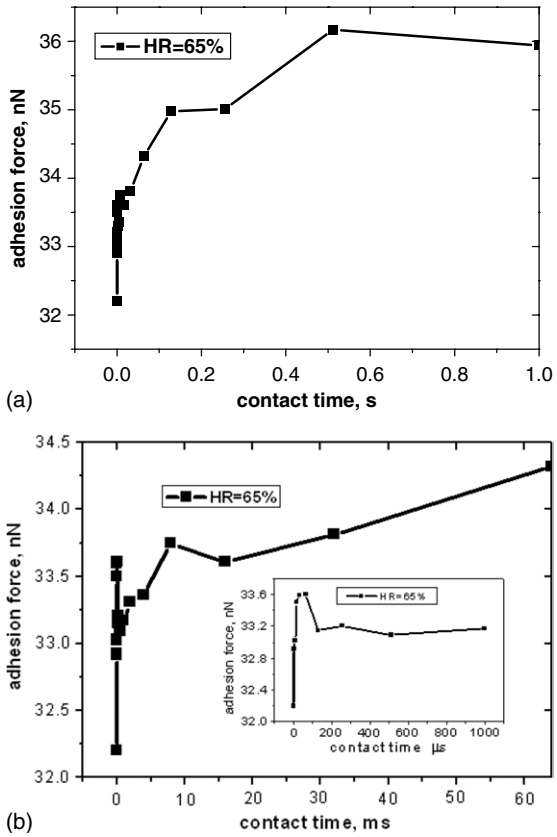

Figure 6. The same data as in figure 1 plotted on a small scale to reveal more details concerning the initial growth of the liquid bridge.

plays a dominant role in the liquid bridge growth. Now the same data as in figure 1 for 65% relative humidity are plotted on a small scale to reveal more detail concerning the initial growth of the liquid bridge in figure 6. Although the peaking force in figure 6(*b*) cannot be explained at present, it is seen that the adhesion force increases sharply in a time range of 0–100 μs. The equilibrium time derived from equation (13), which is plotted in figure 5, is about 1 millisecond, while the time range for the adhesion force to have sharp variation is less than several hundred microseconds. Hence, we believe that the sharp increase of the adhesion force in the initial stage results from the condensation of the water vapour near the contact zone.

4. Conclusion

At ambient conditions, a water neck forms between the AFM tip and the substrate due to capillary condensation and adsorption of thin water films at the surfaces [34, 35], and this capillary force is considered to have a very big influence on surface force measurements and pull-in stability in MEMS and NEMS [12, 13]. Our findings in this paper have direct relevance to the growth of the liquid bridge with respect to the adhesion force variation with the contact time in the force–displacement measurement in the AFM test. Based on our previous work, a growth model for liquid bridge is proposed.

(a) In the AFM adhesion measurement, the development of adhesion force goes through two stages. The first stage

sees a sharp increase of adhesion force with increasing contact time. The second is the process of fairly slow increase of adhesion force with increasing contact time, and it is in this stage that the adhesion force reaches its equilibrium.

(b) Our solution to the condensation model shows that the equilibrium time is mainly the time of the first stage. Hence, the first stage is the process of water vapour condensation near the contact zone between the AFM and the substrate.

(c) Like the first stage, our solution to the motion of the liquid thin film also shows the equilibrium time is mainly the time of this stage. So this stage also is the process of the motion of the liquid thin film to form the liquid bridge.

Acknowledgments

We wish to acknowledge the financial support from the Distinguished Young Scholar Fund of NSFC (Grant No 10225209), key project from the Chinese Academy of Sciences (Grant No KJCX2-SW-L2). The authors are also grateful for the opening funds from the Central Laboratory of Strength and Vibration at Tsinghua University and the Key Lab. of Failure Mechanics (FML), Chinese Ministry of Education, Tsinghua University.

Appendix. (See figure 4)

The volume of liquid bridge

$$V = 2\pi \int_{\theta'}^{\theta} ((a + R_t(1-\cos\psi))R_t \sin\psi R_t \cos\psi)\,\mathrm{d}\psi$$

$$+ 2\pi \int_0^{\pi/2} \left((r_k - r_k\cos\psi)\left(R_t\sin\theta + \sqrt{r_k^2 - [R_t(1-\cos\theta) - h + a]^2} - r_k\sin\psi\right) r_k\cos\psi\right)\mathrm{d}\psi$$

$$\approx 2\pi R_t^2\left(\frac{a}{4} - \frac{h_0}{4} - \frac{R_t}{12} + \frac{1}{4}R_t\cos\theta - \frac{1}{4}a\cos 2\theta + \frac{1}{4}h_0\cos 2\theta - \frac{1}{4}R_t\cos 2\theta + \frac{1}{12}R_t\cos 3\theta\right)$$

$$+ 2\pi r\left(\frac{r_k^2}{6} - \frac{1}{4}(-4+\pi)r_k \times \left(\sqrt{r_k^2 - [R_t(1-\cos\theta) - h_0 + a]^2} + R_t\sin\theta\right)\right),$$

where

$$\cos\theta' = \frac{R_t - h_0 + a}{R_t}.$$

Because in our problem, $a \ll R_t$, $h_0 \ll R_t$, so

$$V = 2\pi R_t^3\left(-\tfrac{1}{12} + \tfrac{1}{4}\cos\theta - \tfrac{1}{4}\cos 2\theta + \tfrac{1}{12}\cos 3\theta\right).$$

Assuming $R_t(1-\cos\theta) + a = h_0 + r_k$, the volume can be rewritten as

$$V = 2\pi R_t^3\left(\frac{1}{4}\frac{R_t + a - h_0 - r_k}{R_t} - \frac{1}{4}\left(2\left(\frac{R_t + a - h_0 - r_k}{R_t}\right)^2 - 1\right) + \frac{1}{12}\left(\frac{R_t + a - h_0 - r_k}{R_t}\left(2\left(\frac{R_t + a - h_0 - r_k}{R_t}\right)^2 - 1\right) - \frac{4(r_k + h_0 - a)}{R_t}\frac{R_t + a - h_0 - r_k}{R_t}\right) - \frac{1}{12}\right)$$

$$= \frac{\pi}{3}(2R_t - r_k - h_0 + a)(r_k + h_0 - a)^2$$

$$\approx \frac{2}{3}\pi R_t(r_k + h_0 - a)^2.$$

Here $h_0 = 0.5$ nm, $a = 0.2$ nm, for the problem of the motion of the liquid, $r_b \gg h_0 - a$, then for this problem, $V \approx \frac{2}{3}\pi R_t r_b^2$.

References

[1] Weisenhorn A L, Hansma P K, Albrecht T R and Quate C F 1989 *Appl. Phys. Lett.* **54** 2651
[2] Israelachvili J N 1992 *Intermolecular and Surface Forces* 2nd edn (San Diego, CA: Academic)
[3] Thundat T, Zheng X Y, Chen G Y and Warmack R J 1993 *Surf. Sci. Lett.* **294** L939
[4] Xiao X D and Qian L M 2000 *Langmuir* **16** 8153
[5] Xu L, Lio A, Hu J, Ogletree D E and Salmeron M 1998 *J. Phys. Chem.* B **102** 540
[6] Sedin D L and Rowlen K L 2000 *Anal. Chem.* **72** 2183
[7] Wei Z and Zhao Y P 2004 *Chin. Phys. Lett.* **21** 616
[8] Tang J, Wang C, Liu M Z, Su M and Bai C L 2000 *Chin. Sci. Bull.* **45** 2612
[9] Gurevich A B, Weldon M K, Chabal Y J, Opila R L and Sapjeta J 1999 *Appl. Phys. Lett.* **74** 1257
[10] Mate C M 1992 *J. Appl. Phys.* **72** 3084
[11] Chilamakuri S and Bhushan B 1999 *J. Appl. Phys.* **86** 4649
[12] Palasantzas G 2006 *J. Appl. Phys.* **100** 054503
[13] Palasantzas G 2007 *J. Appl. Phys.* **101** 053512
[14] Nevshupa R A, Scherge M and Ahmed S I U 2002 *Surf. Sci.* **517** 17
[15] Brauer P, Poosch H R, Szombathely M V, Heuchel M and Jaroniec M 1992 *Proc. 4th Int. Conf. on Fundamentals of Adsorption (Kyoto, Japan)*
[16] Jaroniec M and Madey R 1988 *Physical Adsorption on Heterogeneous Solids* (Amsterdam: Elsevier)
[17] Anderson P J and Horlock R F 1969 *Trans. Faraday Soc.* **65** 251
[18] Israelachvili J N and Adams G E 1978 *J. Chem. Soc. Faraday Trans. 1* **74** 975
[19] Parker J L, Christenson H K and Ninham B W 1989 *Rev. Sci. Instrum.* **60** 3135
[20] Maeda N, Israelachvili J N and Kohonen M M 2003 *Proc. Natl Acad. Sci.* **100** 803
[21] Riedo E, Lévy F and Brune H 2002 *Phys. Rev. Lett.* **88** 185505
[22] Kohonen M M, Maeda N and Christenson H K 1999 *Phys. Rev. Lett.* **82** 4667
[23] Lubarsky G V, Davidson M R and Bradley R H 2006 *Phys. Chem. Chem. Phys.* **8** 2525
[24] Sirghi L, Szoszkiewicz R and Riedo E 2006 *Langmuir* **22** 1093
[25] Beaglehole D and Christenson H K 1992 *J. Phys.Chem.* **96** 3395

[26] de Boer J H 1953 *Dynamical Character of Adsorption* (Oxford: Clarendon)
[27] Dushman S 1949 *Scientific Foundations of Vacuum Technique* (New York: Wiley)
[28] Robert B B 1994 *Growth and Diffusion Phenomena: Mathematical Frameworks and Applications* (Berlin: Springer)
[29] Carslaw H S and Jaeger J C 1959 *Conduction of Heat in Solids* 2nd edn (Oxford: Clarendon)
[30] de Gennes P G, Brochard-Wyart F and Quéré D 2004 *Capillary and Wetting Phenomena* (Berlin: Springer)
[31] Uri Raviv U, Laurat P and Klein J 2001 *Nature* **413** 51
[32] Ackler H D, French R H and Chiang Y M 1996 *J. Colloid Interface Sci.* **179** 460
[33] Binggeli M and Mate C M 1994 *Appl. Phys. Lett.* **65** 415
[34] Butt H J, Cappella B and Kappl M 2005 *Surf. Sci. Rep.* **59** 1
[35] Butt H J, Farshchi-Tabrizi M and Kappl M 2006 *J. Appl. Phys.* **100** 024312